Determination of the Product Branching Fraction for HNF in the Reaction of HN_3 with F

Kevin B. Hewett and D. W. Setser*

Department of Chemistry, Kansas State University, Manhattan, Kansas 66506

Received: July 2, 1997; In Final Form: September 10, 1997[⊗]

The reaction of F atoms with HN_3 forms the products HF ($+N_3$) or HNF ($+N_2$). The product branching fraction for this reaction has been investigated in a room-temperature flow reactor using laser-induced fluorescence to monitor the concentration of HNF. A microwave discharge applied to a dilute flow of CF_4 in argon served as the F atom source. Using reactant concentrations of $(0.7-3.0) \times 10^{12}$ and $(1.7-20.0) \times 10^{12}$ molecules cm^{-3} for CF_4 and HN_3, respectively, the rate constant for formation of HNF from $HN_3 + F$ was determined to be $(6.3 \pm 3.5) \times 10^{-12}$ cm^3 $molecule^{-1}$ s^{-1}. The average product branching fraction for formation of HNF was determined to be $0.03^{+0.02}_{-0.01}$. The quenching rate constant of electronically excited HNF by Ar was determined to be $(3.0 \pm 0.3) \times 10^{-11}$ cm^3 $molecule^{-1}$ s^{-1}. In addition, secondary reactions between HNF and HN_3, F, and H_2S were examined. No reaction was observed to occur between HNF and HN_3. The reaction of HNF + F was observed to occur with an estimated rate constant of 2.0×10^{-10} cm^3 $molecule^{-1}$ s^{-1}. The rate constant for the reaction between HNF and H_2S was found to be less than 1×10^{-12} cm^3 $molecule^{-1}$ s^{-1}.

A. Introduction

The chemical production of the azide radical (N_3) is commonly done using the reaction of fluorine atoms with hydrazoic acid.

$$F + HN_3 \rightarrow N_3 + HF \quad (1)$$

However, an alternative reaction channel, first proposed by Sloan and co-workers[1,2] and later observed experimentally by Chen and Dagdigian,[3] leads to the formation of the HNF radical.

$$F + NH_3 \rightarrow HNF + N_2 \quad (2)$$

The kinetics and reaction dynamics of (1) have been extensively studied.[4−9] The vibrational state distribution of HNF and its deuterated analogue have also been studied, but the branching fraction between (1) and (2) has not been determined. Knowing this fraction is essential if (1) is to serve as a useful source of azide radicals.

In this paper, we examine (2) using laser-induced fluorescence (LIF) detection of HNF with the goal of determining the branching fraction. The HNF fluorescence was calibrated using the LIF of IF generated by the reaction

$$F + CF_3I \rightarrow IF + CF_3 \quad (3)$$

in the same reactor for the same $[F]_0$. The rate constant for reaction (1) has been previously reported[8] to be $(1.1 \pm 0.1) \times 10^{-10}$ cm^3 $molecule^{-1}$ s^{-1}, while the rate constant[10] for (3) is $(1.62 \pm 0.16) \times 10^{-10}$ cm^3 $molecule^{-1}$ s^{-1}. The amount of HNF formed via (2) depends upon the elapsed time between mixing the reagents and observation of the products using LIF. At short times (∼2 ms) the HNF concentration is determined by the extent of reaction. At longer times (∼7−8 ms), the yield of HNF is limited by the branching fraction, since the reaction is complete. We examined both situations under fluorine atom limited reaction conditions and determined the fraction of $[F]_0$ that reacts with HN_3 to form HNF.

The measured concentration of HNF depends not only upon the amount formed during (2) but also upon the amount removed by secondary reactions. The flow reactor contains several species which could possibly react with HNF. Two possible secondary reactions, F + HNF and HN_3 + HNF, were examined by varying the concentrations of F atoms and HN_3 molecules, respectively. Finally, a molecule not normally found in the flow reactor, H_2S, was added to investigate the reactivity of HNF toward H atom abstraction.

B. Experimental Methods

The reactions of F atoms with hydrazoic acid and with trifluoroiodomethane were carried out in a flow reactor at room temperature. The reaction products, HNF or IF, were detected using laser-induced fluorescence. The flow reactor and LIF system used in this work are described below.

Flow Reactor. The flow reactor was a 52 cm long, 50 mm diameter Pyrex tube, which was coated with halocarbon wax to prevent the loss of radicals on the reactor walls. The inlet gas tubes for the Ar buffer gas, the F atom source (CF_4), the reagent (either HN_3 or CF_3I), and the quenching gas (for the H_2S + HNF experiments) were located in an aluminum flange attached via an O-ring joint to the front end of the reactor. Two baffled sidearms, located ∼16 cm from the gas inlet, allowed the laser beam to enter and exit the reactor. The fluorescence was collected through a quartz window located perpendicular to the sidearms. The reactor was pumped using a mechanical pump/blower combination, and a linear flow velocity of 6400 cm s^{-1} was achieved over the pressure range of 0.4−2 Torr. This resulted in a reaction time of 2 ms. By throttling the pump with a gate valve, the flow velocity could be reduced, thus increasing the reaction time from 2 to 8 ms. Alternatively, the reaction time was increased by adding a 30 cm extension to the flow reactor. This extension resulted in a reaction time of ∼7 ms without throttling the pump. When using the extension, an additional inlet tube for H_2S was added to the flange. This

[⊗] Abstract published in *Advance ACS Abstracts,* November 1, 1997.

S1089-5639(97)02156-7 CCC: $14.00

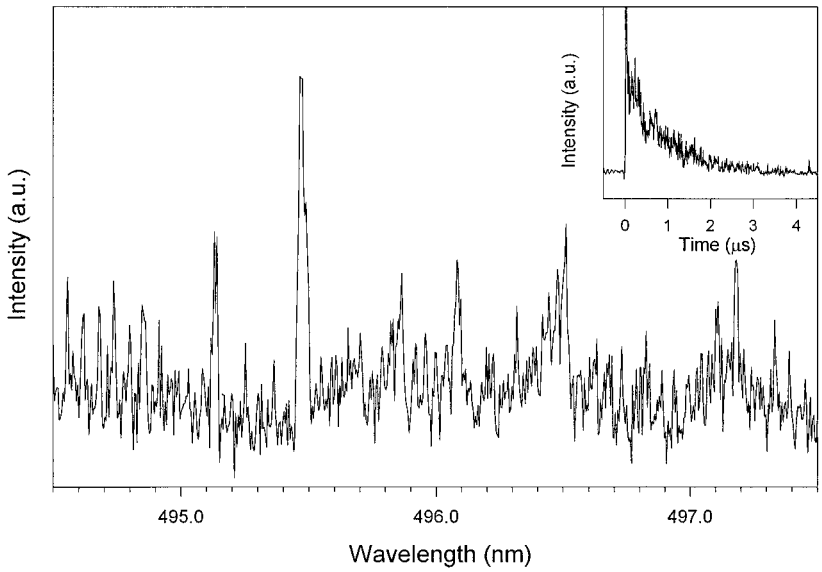

Figure 1. LIF excitation spectrum of the $\tilde{A}\ ^2A'(0,0,0) \leftarrow \tilde{X}\ ^2A''(0,0,0)$ transition of HNF. The reagent concentrations were $[Ar] = 1.6 \times 10^{16}$, $[CF_4] = 1.2 \times 10^{12}$, and $[HN_3] = 3.2 \times 10^{12}$ molecules cm^{-1}. The laser power was 1.4 mJ/pulse, and 64 laser shots were averaged for each data point. The strong spectral feature near 495.5 nm is the $^RQ_0$ branch. The inset in the upper right corner shows a waveform taken by exciting the ^RQ_o branch. The waveform, which is the average of 2048 separate laser shots, gives a decay of $\sim 1\ \mu s$.

inlet tube terminated with a perforated ring perpendicular to the axis of the flow reactor. The inlet tube for H_2S was movable, allowing the time between mixing of the reactants and the quenching gas to be varied.

The argon buffer gas was purified by passage through two cooled (196 K) molecular sieve traps. The F atoms were produced by passing an Ar/CF_4 mixture through a microwave discharge. It has been shown previously that for CF_4 concentrations in the range $(0.2-2.0) \times 10^{12}$ molecules cm^{-3} nearly complete dissociation ($2F + CF_2$) is achieved:[11,12] thus $[F]_0 = 2[CF_4]$ was assumed. The HN_3 was prepared by the reaction of excess stearic acid with sodium azide (NaN_3) heated to 363 K under vacuum. The product, which was collected in a 12 L Pyrex reservoir, was diluted to 10% with argon. The CF_3I and H_2S were taken from commercial vendors and purified via freeze−pump−thaw cycles and stored as mixtures in argon. The flow rates of CF_4, HN_3, CF_3I, and H_2S were controlled by stainless steel needle valves and measured by the pressure rise in a calibrated volume. The argon flow rate was controlled by needle valves and measured by floating-ball flow meters that had been calibrated using a wet test meter.

LIF System. The laser pulse was generated using a Nd:YAG laser (Quantel YG661S) pumped dye laser (Lambda Physik FL 3002) operating at 10 Hz. The laser produced 10 ns pulses with energies of ~ 2 mJ/pulse at 500 nm with a spectral bandwidth of 0.2 cm^{-1} using Coumarin 500 as the dye. The laser beam entered and exited the reactor via Brewster angle quartz windows on the sidearms. The fluorescence was collected using a *f*4.5 condenser lens and focused onto the entrance slit of a 0.3 m monochromator (McPherson 218). A Hammamatsu R955 photomultiplier was attached to the exit slit of the monochromator, and the signal from the PMT was sent to a digital storage oscilloscope (Hewlett-Packard 54522A) operating under computer control.

C. Experimental Results

When the HNF $\tilde{A}^2A'(0,0,0) \leftarrow \tilde{X}^2A''(0,0,0)$ transition was excited (494−498 nm), the wavelength of the monochromator was set to 536.0 nm, thus monitoring the fluorescence back to the $\tilde{X}^2A''(0,1,0)$ state.[13] The waveforms collected by the digital storage oscilloscope were integrated over the time interval of 0.02−4 μs. Figure 1 shows a typical LIF spectrum of HNF and a typical waveform for excitation of the $^RQ_0$ branch of HNF as collected with our apparatus. For IF, the $B\ ^3\Pi_{0+}(v'=2) \leftarrow X\ ^1\Sigma^+(v''=0)$ transition was pumped (505.6−512.0 nm) and the monochromator was set to 522.1 nm, thus monitoring fluorescence to the $X\ ^1\Sigma^+(v''=1)$ state, which should have the largest Franck−Condon factor from the $v' = 2$ level in the B state.[14] The waveforms were integrated over the 0.02−36 μs interval. A typical spectrum of IF and a waveform for excitation of the P(10)/R(18) transition is shown in Figure 2. The intensity of the strongest spectral features in the IF(B−X) spectrum is ~ 10 times as intense as the strongest feature (the $^RQ_0$ branch) of the HNF spectrum. For both HNF and IF, the fluorescence intensities were determined by scanning the laser over each spectral feature, the $^RQ_0$ branch and the P(10)/R(18) transitions for HNF and IF, respectively, and integrating to determine the band area. The spectral intensities were examined as a function of laser power. This demonstrated that the transitions examined for HNF and IF were not saturated under our experimental conditions.

C.1. Comparison of IF and HNF Concentrations. To determine the relative concentrations of HNF formed by (2), the fluorescence was compared to that of IF generated by (3). This comparison was made in two different kinetic regimes. The first case used a short reaction time, and the ratio of concentrations for pseudo-first-order kinetics is determined by

$$\frac{[IF]}{[HNF]} = \frac{[F]_0\,(1 - e^{-k_3[CF_3I]\Delta t})}{[F]_0 \dfrac{k_2}{k_1 + k_2}(1 - e^{-(k_1+k_2)[HN_3]\Delta t})} \qquad (4)$$

where k_1, k_2, and k_3 are the rate constants for (1), (2), and (3), respectively, and Δt is the reaction time. The second case uses long reaction times, and the ratio of IF to HNF is limited by the branching fraction between (1) and (2). In this case, the product [reagent]Δt is large, and the right-hand side of (4) reduces to $(k_1 + k_2)/k_2$. The ratio of the LIF intensities of HNF and IF was measured in order to determine the ratio of the concentrations, which in turn gives the branching ratio $k_2/(k_1 + k_2)$.

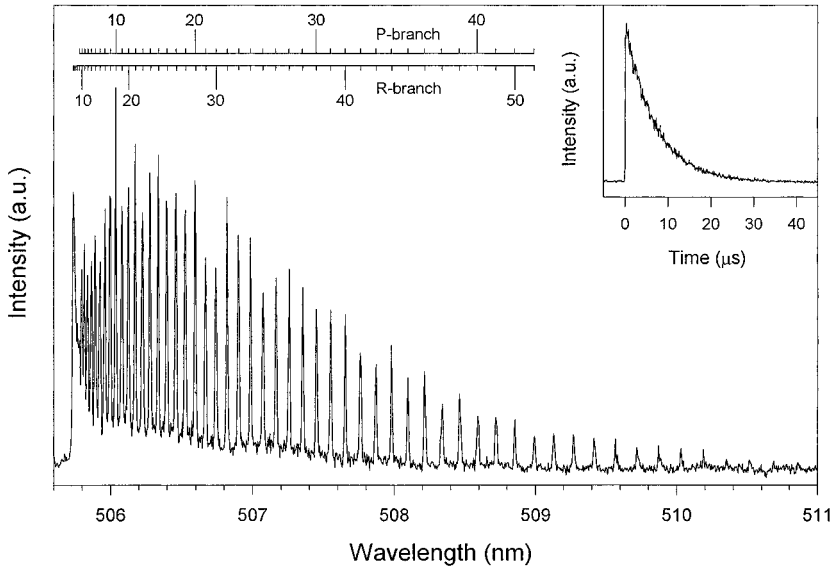

Figure 2. LIF excitation spectrum of the B $^3\Pi_{0+}(v'=2) \leftarrow$ X $^1\Sigma^+(v''=0)$ transition of IF. The reagent concentrations were [Ar] = 1.6×10^{16}, [CF_4] = 1.2×10^{12}, and [CF_3I] = 3.2×10^{12} molecules cm^{-3}. The laser power was 1.7 mJ/pulse, and 32 laser shots were averaged for each data point. The inset at the upper right shows a waveform taken by exciting the P(10)/R(18) transitions. The waveform, which was the average of 2048 separate laser shots, gives a lifetime of 7.2 μs.

TABLE 1: Reagent Concentrations and Measured Integrated Intensities Used To Investigate Reaction 2. At Short Reaction Times (2 ms), the Rate Constant k_2 Can Be Extracted from the Ratio of HNF and IF Concentrations. The Average Value of k_2 is (6.3 ± 3.5) × 10^{-12} cm^3 molecule^{-1} s^{-1}. At Long Reaction Times (7.8 ms) the Ratio of HNF and IF Concentrations Is Equal to the Branching Fraction. The Average Branching Fraction Is $0.03^{+0.02}_{-0.01}$

reagent concentrations (10^{12} molecules cm^{-3})				reaction	intensity					
[Ar]	[CF_4]	[HN_3]	[CF_3I]	time (ms)	HNF[a]	IF[b]	$n_{HNF,k}/n_{IF,i}$	[HNF]/[IF]	k_2 (10^{-12} cm^3 molecule^{-1} s^{-1})	branching fraction
15 500	1.2	3.2	3.2	2.0	0.035	0.18	0.122	0.0327	4.66	
15 400	0.72	3.4	3.4	2.0	0.038	0.15	0.158	0.0425	6.03	
15 800	0.74	1.7	1.7	2.0	0.044	0.12	0.232	0.0623	9.45	
15 900	1.5	3.3	3.3	2.0	0.045	0.24	0.119	0.0320	4.53	
16 000	1.5	4.9	4.9	2.0	0.049	0.17	0.184	0.0493	6.72	
62 100	2.45	20	20	7.8	0.017	0.16	0.148	0.0396		0.040
62 000	2.45	13	13	7.8	0.015	0.17	0.122	0.0329		0.033
62 000	2.45	11.8	11.8	7.8	0.013	0.16	0.113	0.0303		0.030
62 000	2.45	6.7	6.7	7.8	0.012	0.16	0.104	0.0279		0.028

[a] Integrated intensity from excitation of the $^RQ_0$ branch of HNF. [b] Integrated intensity from excitation of the P(10) and R(18) transitions of IF.

The measured LIF intensities of IF and HNF are given in Table 1 for a variety of experimental conditions. The areas of the spectral features, namely the $^RQ_0$ branch of HNF and the P(10)/R(18) peak for IF, were measured. We can determine either the rate constant k_2 or the branching fraction for (1) and (2) by comparing the ratio of [HNF] to [IF].

Quenching of HNF. Detection of the laser-induced fluorescence of the HNF molecule was initially attempted with reagent flow rates of 0.21, 0.56, and 3337.7 μmol/s of CF_4, HN_3, and Ar, respectively, and a total reactor pressure of 0.5 Torr. Under these conditions, the measured lifetime for the $^RQ_0$ branch was 1.0 μs, a factor of 3 shorter than the previously reported value of 3.6 μs.[3] Further investigations into the reduced lifetime were performed by changing the argon pressure in the reactor. Figure 3 shows the Stern−Volmer plot of $1/\tau$ vs pressure. The plot is linear with pressure, and upon extrapolating to zero pressure we obtain a lifetime of 3.9 ± 0.3 μs, which is within the experimental error of the previously reported value. Furthermore, the quenching rate constant obtained for Ar is (3.0 ± 0.3) × 10^{-11} cm^3 molecule^{-1} s^{-1}. The estimate for the uncertainty includes the flow time as well as the least-squares uncertainty in the quenching plot.

C.2. Conversion of Relative LIF Intensities of IF and HNF to Relative Concentrations. The fluorescence intensity of a nonsaturated transition of IF can be represented as

$$I_{IF} = n_{IF,i}\sigma_{IF,ij}VL\Theta\left[\frac{A_{jl}}{A_{jl} + \sum A_{jm} + k_d + \sum k_q[M_q]}\right]_{IF} \quad (5)$$

where $n_{IF,i}$ is the number of IF(X) molecules in the ith state, $\sigma_{IF,ij}$ is the absorption cross section for the transition between the ith and jth states, V is the imaging volume, L is the laser power, Θ is the light collection efficiency of the optics, A_{jl} is the Einstein coefficient for spontaneous emission between states, $\sum A_{jm}$ is the sum of Einstein coefficients for undetected emission, k_d is the predissociation rate constant, and the $k_q[M_q]$ term represents the sum of electronic quenching and vibrational relaxation. Similarly, the fluorescence intensity of HNF can be represented as

$$I_{HNF} = n_{HNF,k}\sigma_{HNF,kj}VL'\Theta\left[\frac{A_{jl}}{A_{jl} + \sum A_{jm} + k'_d + \sum k'_q[M'_q]}\right]_{HNF} \quad (6)$$

where $n_{HNF,k}$ is the number of HNF($\tilde{X}$) molecules in the kth state. The ratio of (5) and (6) allows the experimental parameters V and Θ to be eliminated, resulting in the following

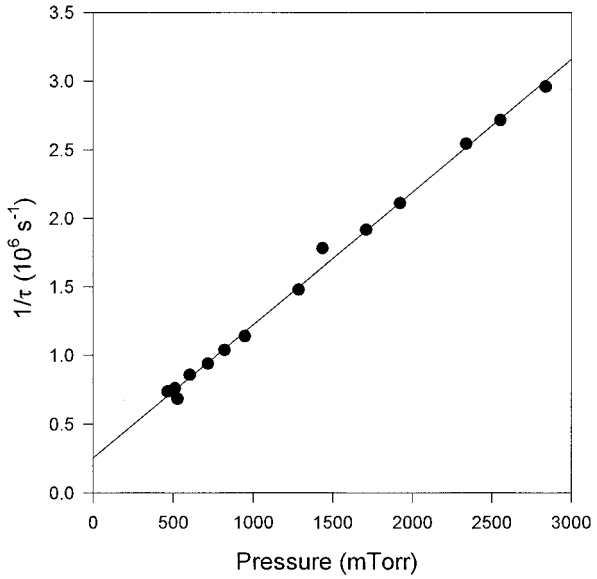

Figure 3. Stern−Volmer plot of the inverse lifetime of HNF(Ã) vs pressure. The pressure was increased by adding Ar to the reactor. The radiative lifetime, obtained by extrapolating to zero pressure, was determined to be 3.9 ± 0.3 μs. The quenching rate constant for HNF(Ã) with Ar was determined to be (3.0 ± 0.3) × 10^{-11} cm^3 $molecule^{-1}$ s^{-1} from the slope.

expression for the ratio of HNF molecules to IF molecules excited by the laser.

$$\frac{n_{\mathrm{HNF},k}}{n_{\mathrm{IF},i}} = \frac{L}{L'}\frac{I_{\mathrm{HNF}}}{I_{\mathrm{IF}}}\frac{\sigma_{\mathrm{IF},ij}}{\sigma_{\mathrm{HNF},kj}}\left[\frac{A_{jl}+\sum A_{jm}+k_{\mathrm{d}}'+\sum k_{\mathrm{q}}'[\mathrm{M}_{\mathrm{q}}']}{A_{jl}}\right]_{\mathrm{HNF}} \times \left[\frac{A_{jl}}{A_{jl}+\sum A_{jm}+k_{\mathrm{d}}+\sum k_{\mathrm{q}}[\mathrm{M}_{\mathrm{q}}]}\right]_{\mathrm{IF}} \quad (7)$$

The ratio of HNF molecules to IF molecules in the specific states denoted by k and i is determined by multiplying the measured intensity ratio by a series of factors that can be ascertained.

The predissociation rate constants for IF and HNF have been previously determined. Clyne and McDermid have demonstrated that IF(B $^3\Pi_{0+}$) does not predissociate unless it is excited above the $v' = 8$, $J = 52$ state.[15] Since in this work we did not excite IF above $v' = 2$, the predissociation rate constant for IF, k_{d}, is equal to zero. Similarly, Chen and Dagdigian have shown that the lowest vibrational levels of HNF($\tilde{A}^2A'$) do not predissociate:[3] thus k_{d}' is also equal to zero.

The sum of the Einstein A coefficients for IF from the B $^3\Pi_{0+}(v'=2)$ state to the ground state is equal to the reciprocal of the radiative lifetime; $\tau_{\mathrm{rad}} = 7.1$ μs, $\Sigma A = 140\,845$ s^{-1}. Using the data of Clyne and McDermid,[15] the A_{jl} coefficient for the B $^3\Pi_{0+}(v'=2) \leftarrow X^1\Sigma^+(v''=1)$ transition being monitored is calculated to be 30 745 s^{-1}. Accordingly, in (7) the $A_{jl} = 30\,745$ s^{-1} and $\Sigma A_{jm} = 110\,100$ s^{-1}. For HNF, the individual Einstein A coefficients are not known. However, from chemiluminescence studies[13] we know that emission from the $\tilde{A}^2A'(0,0,0)$ level only occurs to four ground-state levels; those with $v_2'' =$ 0, 1, 2, and 3. Furthermore, the Franck−Condon factors have been calculated by Peric et al.[16] using theoretical models. This allows the relative magnitudes of the A coefficients to be determined. Using this together with the radiative lifetime, $\tau_{\mathrm{rad}} = 3.6$ μs, for the $\tilde{A}^2A'(0,0,0)$ state as determined by Chen and Dagdigian,[3] the A_{jl} coefficient for the monitored transition $\tilde{A}^2A'(0,0,0) \leftarrow \tilde{X}^2A''(0,1,0)$ is estimated to be ~39% of the $\Sigma A = 277\,778$ s^{-1}. As a result, we use $A_{jl} = 107\,500$ s^{-1} and $\Sigma A_{jm} = 170\,278$ s^{-1} in (7).

Quenching of IF(B) has been studied with a variety of quenching partners. Using Ar as the bath gas, the quenching rate constant of IF(B $^3\Pi_{0+}$) was determined by Wolf and Davis[17] to be less than 1 × 10^{-14} cm^3 $molecule^{-1}$ s^{-1}. Furthermore, the vibrational relaxation rate constant[18] of IF(B) in Ar is on the order of 1 × 10^{-12} cm^3 $molecule^{-1}$ s^{-1}, and neither vibrational relaxation nor quenching is important for our experiments. As previously discussed, the quenching rate constant for HNF(Ã) with Ar was examined and was found to be (3.0 ± 0.1) × 10^{-11} cm^3 $molecule^{-1}$ s^{-1}.

The final terms needed to determine the HNF concentration excited by the laser are the relative absorption cross sections for IF and HNF; these will be obtained from the radiative lifetimes. The integrated absorption cross section may be written in terms of the oscillator strength as

$$\int \sigma_v \, \mathrm{d}\nu = f\frac{\pi e^2}{mc} \quad (8)$$

where c is the speed of light, m and e are the mass and charge on an electron, respectively, and f is the oscillator strength. The oscillator strength, including both rotation and vibration, can be written as

$$f = \frac{A_{ij}mc}{8e^2\pi^2\nu^2}\frac{S(J',J'')}{2J''+1} \quad (9)$$

where $S(J',J'')$ are the Hönl−London factors and J'' is the ground-state rotational quantum number. Combining (8) and (9), we obtain the following expression for the integrated absorption cross section:

$$\int \sigma_v \, \mathrm{d}\nu = \frac{A_{ij}}{8\pi\nu^2}\frac{S(J',J'')}{2J''+1} \quad (10)$$

The ratio of integrated absorption cross sections becomes (11).

$$\frac{\int \sigma_{\mathrm{IF},v}\,\mathrm{d}\nu}{\int \sigma_{\mathrm{HNF},v}\,\mathrm{d}\nu} = \frac{A_{\mathrm{IF},ij}}{A_{\mathrm{HNF},kl}}\frac{\nu^2_{\mathrm{HNF}}}{\nu^2_{\mathrm{IF}}}\left[\frac{S(J',J'')}{2J''+1}\right]_{\mathrm{IF}}\left[\frac{2J''+1}{S(J',J'')}\right]_{\mathrm{HNF}} \quad (11)$$

The formulas given by Herzberg[19] for the Hönl−London factors for the R and P branches of a diatomic with $\Delta\Lambda = +1$, as is the case with the B $^3\Pi_{0+}(v'=2) \leftarrow X\,^1\Sigma^+(v''=0)$ transition of IF, are reproduced below:

$$S(J''+1,J'') = \frac{(J''+2+\Lambda'')(J''+1+\Lambda'')}{4(J''+1)}$$

$$S(J''-1,J'') = \frac{(J''-1-\Lambda'')(J''-\Lambda'')}{4J''} \quad (12)$$

Using (12), the $S(J',J'')$ for the P(10) and R(18) transitions of IF were calculated. A weighted average of $S(J',J'')/(2J''+1)$ was used in (11). The weights were obtained from the relative populations of the P(10) and R(18) lines as determined from a 300 K Boltzmann distribution.

A similar calculation may be made for HNF if it is treated as a symmetric top molecule, which is possible since the ground-state rotational constants of HNF, as determined by Woodman,[20] are 17.688, 1.0389, and 0.9777 cm^{-1} for A, B, and C, respectively. The Hönl−London formula[21] for a R subband of a perpendicular band of a symmetric top molecule is given by

$$S(J'',J'') = \frac{(J'' + 1 + K'')(J'' - K'')}{J''(J'' + 1)} \qquad (13)$$

For the $^{R}Q_0$ branch of HNF, (13) is always equal to 1 since $K'' = 0$. The rotational contribution for HNF to (11) is thus $1/(2J'' + 1)$. The fluorescence intensity of HNF was determined by scanning over the $^{R}Q_0$ branch and measuring the area. As a result, all rotational levels are excited and contribute to the measured intensity. A 300 K Boltzmann distribution was calculated for a symmetric top molecule with rotational constants equal to A and $\bar{B} = (B + C)/2$. A weighted average was used for $J'' = 1-40$ with the relative populations used as the weights. The ratio of the integrated absorption cross sections is calculated using (11) to be 0.363 using the frequencies and previously determined Einstein A coefficients.

For the final calculation the fraction of molecules in states i and k that are excited by the laser is needed. The nascent IF vibrational population distribution from (3) has been determined using LIF in a crossed molecular beam experiment.[22] To characterize the vibrational distribution in our flow reactor, the LIF from $v'' = 0$, 1, and 2 were recorded. The IF($\tilde{X}$) vibrational distribution was found to be relaxed with 300 K Boltzmann population ratios. The vibrational relaxation rate of IF(v) is fast compared to the ~2 ms residence time before LIF probing. As a result, we used a 300 K Boltzmann distribution where 87% of the IF molecules are in the $v = 0$ state. We excited two rotational transitions, the P(10) and the R(18), which are overlapped with one another. The sum of the rotational population, for a Boltzmann distribution at 300 K, for $J = 10$ and 18 is ~5.0% of the IF molecules in the ground vibrational state. As a result, 4.4% of the total number of IF molecules formed in (3) are probed by the laser.

The vibrational distribution of HNF formed by (2) is not known: however, Chen and Dagdigian[3] stated that HNF was vibrationally relaxed in their low-pressure (2 mTorr) experiment. If HNF has a thermal vibrational distribution, then 95% of the molecules are in the (0,0,0) state. An excitation spectrum of the $\tilde{A}^2A'(0,0,0) \leftarrow \tilde{X}^2A''(0,0,0)$ transition of HNF is shown in Figure 1. The rotational transitions that are pumped are those in the $^{R}Q_0$ band, which are overlapped in the spectrum. The width of this spectral feature is ~5 cm^{-1}. Although the bandwidth of our laser is 0.2 cm^{-1}, we scanned the entire $^{R}Q_0$ branch. Treating HNF as a near prolate symmetric top, the rotational population was calculated for a 300 K Boltzmann distribution. Approximately ~16.4% of the molecules have $K'' = 0$ and are accessible to the laser.

Thus, (7) allows one to determine the ratio of HNF molecules that are excited by the laser relative to the number of IF molecules excited by the laser. Since 4.4% of the IF molecules and 16.4% of the HNF molecules are accessible to the laser pulse of light, the ratio determined by (7) can be scaled to the total ratio of HNF and IF molecules.

Comparison of IF and HNF Concentrations. The integrated LIF intensities of IF and HNF for the same $[F]_0$ were recorded. A variety of reactant concentrations, as shown in Table 1, were used. Using the data collected with a reaction time of ~8 ms, the branching fraction for HNF in the reaction of HN_3 with F was determined for each set of initial reactant concentrations. The average branching fraction was found to be $0.03^{+0.02}_{-0.01}$. Using the data collected with a reaction time (Δt) of approximately 2 ms, and comparing the ratio of IF to HNF concentrations obtained from (7), the rate constant k_2 was calculated. Using the known values of k_1 and k_3, the rate constant k_2 was determined to be $(6.3 \pm 3.5) \times 10^{-12}$ cm^3 $molecule^{-1}$ s^{-1}. The two sets of data, at short and long reaction times, can be compared to one another. From the experimentally determined value of k_2 and the value of k_1 reported by Habdas et al.[8] the branching fraction may be calculated. The branching fraction calculated in this way is 0.05, in close agreement with the value determined from long reaction times.

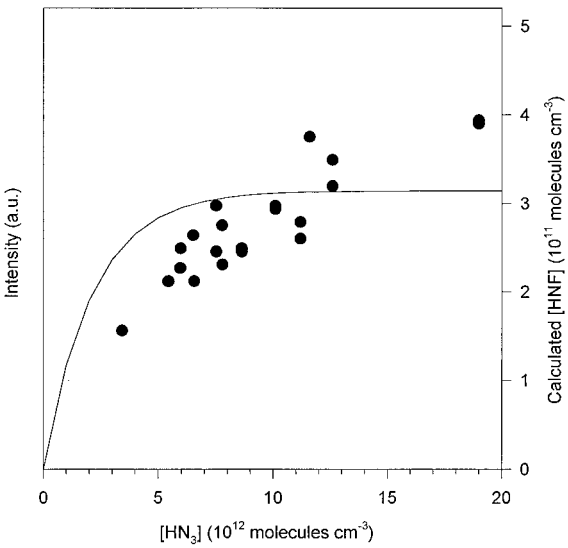

Figure 4. Intensity of the HNF($\tilde{A}$) fluorescence as a function of HN_3 concentration. The reagent concentrations were $[Ar] = 6.3 \times 10^{16}$ and $[CF_4] = 2.9 \times 10^{12}$ molecules cm^{-3}. The measured HNF($\tilde{A}$) fluorescence intensity (●) rises as the HN_3 concentration increases. The calculated HNF concentration from the reaction of F + HN_3 (—) with a reaction time of 5 ms, assuming pseudo-first-order kinetics in HN_3, is given for comparison. No evidence of a decrease in the concentration of HNF is observed, and hence, no reaction between HNF and HN_3 occurs under these reaction conditions.

The uncertainties given for both k_2 and the branching fraction were calculated by propagating the uncertainty in the measured data and the input parameters. The most significant source of potential error is the uncertainty of the relative absorption cross sections for IF and HNF, which was determined to be 0.36 ± 0.18. Other important sources of error are the measurement of the LIF intensity and the Einstein A coefficients for HNF.

C.3. Determination of Reaction Rate Constants of HNF. In addition to the formation rate constant of HNF from HN_3 and F atoms, it is necessary to understand the secondary reactions of HNF that might remove it from the reactor. Several possible reactions of HNF, produced via (2), were examined. These included reactions with HN_3, F atoms, and H_2S. Each of these possible reactions is discussed below.

HNF + HN_3. The possibility that HNF reacted with HN_3 in the reactor was examined under fluorine atom limited reaction conditions by varying the amount of HN_3 in the reactor while keeping the fluorine atom concentration constant. The reaction time was 5.1 ms. As shown in Figure 4, the HNF fluorescence rises as the HN_3 concentration increases. Once the HN_3 concentration exceeds ~8×10^{12} molecule cm^{-3}, the reaction of F + HN_3 should be complete. The apparent further increase in HNF concentration is due to scatter in the experimental data. No evidence was found for a decrease in HNF concentration as a result of added HN_3.

HNF + F. Another possible secondary reaction is that between HNF and F atoms. This reaction was studied by increasing the amount of CF_4, and hence F atoms, passing through the microwave discharge while maintaining a constant HN_3 concentration. The HNF fluorescence observed for $\Delta t =$ 7.0 ms decreased at high CF_4 concentrations, as shown in Figure 5. Since the experimentally measured lifetime of HNF($\tilde{A}^2A'$) did not change, the decrease in fluorescence is due to the

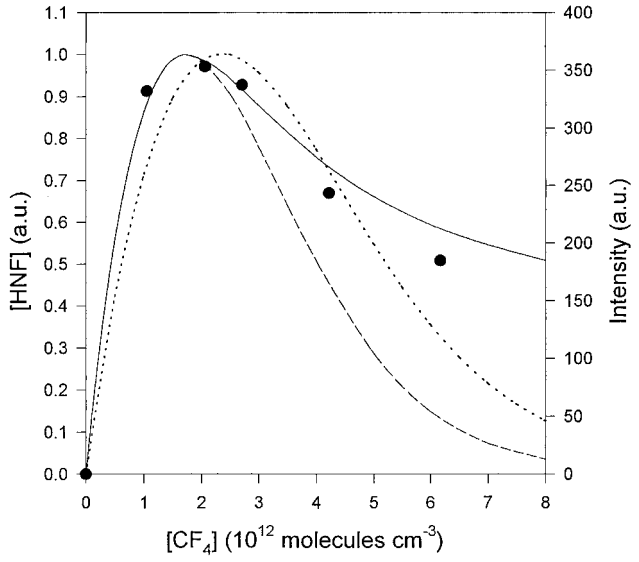

Figure 5. Intensity of HNF fluorescence as a function of added CF_4. The reagent concentrations were [Ar] = 1.8×10^{16} and [HN_3] = 5.2×10^{12} molecules cm^{-3}. The experimental results (●) show that increasing the CF_4 concentration, and hence increasing the F atom concentration, reduces the amount of HNF. The lines indicate various fits from the kinetic models described in the text. Using a constant CF_4 dissociation and HNF + F rate constants of 1.0×10^{-10} (···) or 2.0×10^{-10} (- - -) cm^3 $molecules^{-1}$ s^{-1}, model fits to the data were obtained, but these fits are not adequate representations of the data. Using a variable CF_4 dissociation efficiency and a rate constant of 2.0×10^{-10} (—) cm^3 $molecules^{-1}$ s^{-1}, the kinetic model adequately represents the experimental data.

TABLE 2: Reactions Used To Model the Reaction of F Atoms with HNF. Unless Otherwise Noted All Rate Constants Were Obtained from the NIST Kinetics Database [Ref 24]

reaction	rate constant (cm^3 $molecules^{-1}$ s^{-1})
$F + N_3 \rightarrow NF(a) + N_2$	5.8×10^{-11}
$F + HN_3 \rightarrow HF + N_3$	1.1×10^{-10} [a]
$N_3 + N_3 \rightarrow N_2 + N_2 + N_2$	1.4×10^{-12}
$2NF(a) \rightarrow N_2 + 2F$	5.0×10^{-12} [b]
$F + CF_2 \rightarrow CF_3$	1.3×10^{-11}
$F + CF_3 \rightarrow CF_4$	2.0×10^{-11}
$F + HN_3 \rightarrow HNF + N_2$	4.2×10^{-12} [c]
$F + HNF \rightarrow HF + NF(a)$	2.0×10^{-10} [c]

[a] Reference 8. [b] Reference 25. [c] This work; see text.

removal of HNF($\tilde{X}$) by (14). The most likely products are HF + NF(a $^1\Delta$) following the recombination to give HNF_2.

$$HNF + F \rightarrow \text{products} \qquad (14)$$

To obtain an estimate of the rate constant for (14), we fitted the experimental data using a kinetic model. The reactions used in the model are found in Table 2 along with their rate constants. The first attempts at kinetic modeling assumed that the dissociation of CF_4 in the microwave discharge was constant, always yielding two F atoms and a CF_2 radical. The best fit for the HNF + F rate constant using this assumption was a value between 1×10^{-10} and 2×10^{-10} cm^3 $molecule^{-1}$ s^{-1}. Both of these fits are shown in Figure 5, and neither adequately describes the experimental results. Below CF_4 concentrations of 2×10^{12} molecules cm^{-3}, the experimental data can be adequately fit using the rate constant $k_{14} = 2 \times 10^{-10}$ cm^3 $molecule^{-1}$ s^{-1}, but at higher CF_4 concentrations the model calculations suggest that the HNF concentration should be lower than the observed value. Similarly, if one uses $k_{14} = 1 \times 10^{-10}$ cm^3 $molecule^{-1}$ s^{-1}, the model fits neither the low or the high CF_4 concentration regions adequately, but it is the overall best fit to the data. The probable failure of the model results from the assumption of constant CF_4 dissociation efficiency, which is known[11,12] to decrease from a value of two F atoms from each CF_4 toward one F atom for each CF_4 as the concentration increases from 2.0×10^{12} to approximately 1.0×10^{13} molecules cm^{-3}.

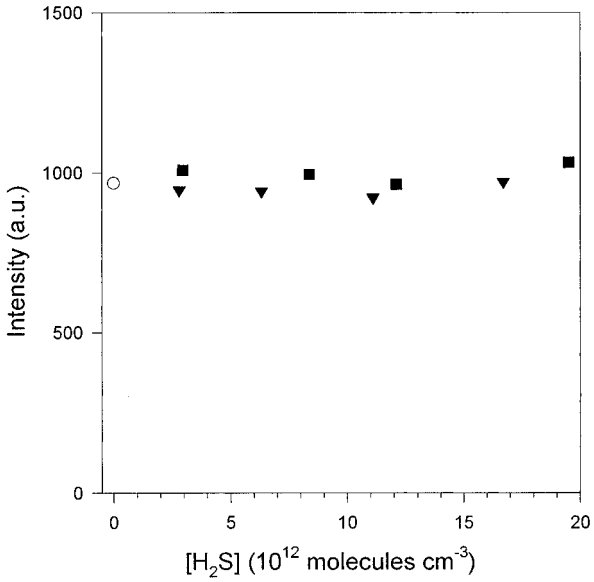

Figure 6. Addition of H_2S to the reactor had no effect upon the HNF fluorescence intensity. The reagent concentrations were [Ar] = 1.8×10^{16}, [CF_4] = 1.1×10^{12}, and [HN_3] = 7.2×10^{12} molecules cm^{-3}. The data shown are for no H_2S (○), for H_2S with a reaction time of 5 ms (▼), and for H_2S with a reaction time of 2 ms (■). Within experimental uncertainty, all three data sets have the same HNF(Ã) fluorescence intensity.

The F atom concentration used in the kinetic model was changed to more accurately reflect the expected CF_4 dissociation. When the CF_4 concentration was below 2.0×10^{12}, the dissociation yields two F atoms for each CF_4. Above 1.0×10^{13}, the dissociation yields only a single F atom. Between these two regimes, the F atom concentration was calculated from a fit to a third-order polynomial [F] = $2.42[CF_4] - 2.56 \times 10^{-13}[CF_4]^2 + 1.14 \times 10^{-26}[CF_4]$.[3] Using this new assumption about the dissociation efficiency of CF_4, the kinetic model fitted the experimental data. The best fit was $k_{14} = 2.0 \times 10^{-10}$ cm^3 $molecule^{-1}$ s^{-1}. The uncertainty is probably ±50%.

HNF + H_2S. The final secondary reaction that was studied was that between HNF and H_2S. The goal was to investigate the reactivity of HNF toward H atom abstraction. H_2S was added to the flow reactor downstream of the HN_3 and F atom inlets. This allowed (1) and (2) to proceed before the H_2S could scavenge the F atoms. As shown in Figure 6, the HNF fluorescence intensity was not affected by the introduction of H_2S. Furthermore, changing the position where the H_2S entered the reactor, and thus altering the reaction time between HNF and H_2S between 2 and 5 ms, also made no difference in the HNF fluorescence intensity. An upper limit for the rate constant is determined in the following way. At the maximum H_2S concentration used, 2×10^{13} molecules cm^{-3}, and a 5 ms reaction time, a 10% decrease in the HNF concentration would require that the rate constant for HNF + H_2S be smaller than $\sim 1 \times 10^{-12}$ cm^3 $molecule^{-1}$ s^{-1}. Since no such decrease was observed, the true rate constant must be less than this value.

D. Conclusion

The reaction of F atoms with HN_3, via (1) or (2), forms the products HF or HNF. Over a variety of initial reactant

conditions, we have determined the average product branching fraction for HNF formation to be $0.03^{+0.02}_{-0.01}$. The rate constant for (2) is $k_2 = (6.3 \pm 3.5) \times 10^{-12}$ cm^3 molecule^{-1} s^{-1}. Electronically excited HNF $\tilde{A}^2A'(0,0,0)$ is quenched by argon with a rate constant of $(3.0 \pm 0.3) \times 10^{-11}$ cm^3 molecule^{-1} s^{-1}. Several possible secondary reactions of HNF were studied. No reaction occurs between HNF and HN_3 or H_2S, but a reaction does occur between HNF and F atoms. The latter reaction occurs with an estimated rate constant of $\sim 2 \times 10^{-10}$ cm^3 molecule^{-1} s^{-1}. By analogy with the H + NF_2 reaction,[23] the products are probably HF + NF(a $^1\Delta$) following the dissociation of HNF_2.

Acknowledgment. This work was supported by the U.S. Air Force under Grant F49620-96-1-0110 from the Air Force Office of Scientific Research. We wish to acknowledge the assistance of Mr. Boris Nizamov, who performed the preliminary experiments to identify the presence of HNF.

References and Notes

(1) Sloan, J. J.; Watson, D. G.; Wright, J. S. *Chem. Phys.* **1979**, *43*, 1−8.
(2) Sloan, J. J.; Watson, D. G.; Wright, J. S. *Chem. Phys.* **1981**, *63*, 283−292.
(3) Chen, J.; Dagdigian, P. J. *J. Chem. Phys.* **1992**, *96*, 7333−7343.
(4) Pritt, A. T., Jr.; Patel, D.; Coombe, R. D. *Int. J. Chem. Kinet.* **1984**, *16*, 977−993.
(5) David, S. J.; Coombe, R. D. *J. Phys. Chem.* **1985**, *89*, 5206−5212.
(6) David, S. J.; Coombe, R. D. *J. Phys. Chem.* **1986**, *90*, 3260−3263.
(7) Liu, X.; MacDonald, M. A.; Coombe, R. D. *J. Phys. Chem.* **1992**, *96*, 4907−4912.
(8) Habdas, J.; Wategaonkar, S.; Setser, D. W. *J. Phys. Chem.* **1987**, *91*, 451−458.
(9) Beaman, R. A.; Nelson, T.; Richards, D. S.; Setser, D. W. *J. Phys. Chem.* **1987**, *91*, 6090−6092.
(10) Iyer, R. S.; Rowland, F. S. *J. Phys. Chem.* **1981**, *85*, 2493−2497.
(11) Du, K. Y.; Setser, D. W. *J. Phys. Chem.* **1991**, *95*, 4728−4735.
(12) Du, K. Y.; Setser, D. W. *J. Phys. Chem.* **1992**, *96*, 2553−2561.
(13) Lindsay, D. M.; Gole, J. L.; Lombardi, J. R. *Chem. Phys.* **1979**, *37*, 333−342.
(14) Clyne, M. A. A.; McDermid, I. S. *J. Chem. Soc., Faraday Trans. 2* **1976**, *72*, 2242−2251.
(15) Clyne, M. A. A.; McDermid, I. S. *J. Chem. Soc., Faraday Trans. 2* **1978**, *74*, 1644−1661.
(16) Peric, M.; Peyerimhoff, S. D.; Buenker, R. J. *Can. J. Chem.* **1983**, *61*, 2500−2505.
(17) Wolf, P. J.; Davis, S. J. *J. Chem. Phys.* **1985**, *83*, 91−99.
(18) Wolf, P. J.; Davis, S. J. *J. Chem. Phys.* **1987**, *87*, 3492−3508.
(19) Herzberg, G. *Molecular Spectra and Molecular Structure. I. Spectra of Diatomic Molecules*; Krieger: Malabar, FL, 1989.
(20) Woodman, C. M. *J. Mol. Spectrosc.* **1970**, *33*, 311−344.
(21) Herzberg, G. *Molecular Spectra and Molecular Structure. III. Electronic Spectra and Electronic Structure of Polyatomic Molecules*; Krieger: Malabar, FL, 1991.
(22) Stein, L.; Wanner, J.; Walther, H. *J. Chem. Phys.* **1980**, *72*, 1128−1137.
(23) Malins, R. J.; Setser, D. W. *J. Phys. Chem.* **1981**, *85*, 1342−1349.
(24) Mallard, W. G.; Westley, F.; Herron, J. T.; Hampson, R. F.; Frizzell, D. H. *NIST Chemical Kinetics Database*, 5.0 ed.; NIST Standard Reference Data: Gaithersburg, MD 20899, 1993.
(25) Du, K. Y.; Setser, D. W. *J. Phys. Chem.* **1990**, *94*, 2425−2435.